A self-consistent theory for seabed volume scattering

Brian H. Tracey and , and Henrik Schmidt

Citation: The Journal of the Acoustical Society of America **106**, 2524 (1999); doi: 10.1121/1.428084
View online: http://dx.doi.org/10.1121/1.428084
View Table of Contents: http://asa.scitation.org/toc/jas/106/5
Published by the Acoustical Society of America

A self-consistent theory for seabed volume scattering

Brian H. Tracey[a] and Henrik Schmidt
Department of Ocean Engineering, Massachusetts Institute of Technology, Cambridge, Massachusetts 02139

(Received 20 April 1998; accepted for publication 8 July 1999)

A self-consistent perturbation method for three-dimensional acoustic scattering due to sound speed and density fluctuations is developed below. This method allows calculation of mean-field attenuation due to scattering, as well as second-moment statistics of the scattered field. Scattering from an inhomogeneous sediment bottom in shallow water is considered as an application. The power spectral density of the scattered field is calculated and used to study the effects of fluctuation statistics. Modal attenuation due to scattering is then calculated for several shallow-water scenarios. The scattering loss calculation is straightforward and is suitable for use with standard normal-mode codes. Numerical results show the influence of the statistical model used to represent bottom randomness and demonstrate the importance of scattering into the continuous spectrum. Scattering loss predictions are shown to agree well with a previous wave number-integration approach. [S0001-4966(99)04610-X]

PACS numbers: 43.30.Bp, 43.30.Ft, 43.30.Gv [DLB]

INTRODUCTION

Volume fluctuations in the ocean are known to strongly affect acoustic propagation. In deep water, the strongest effects come from oceanographic mixing and internal waves, while in shallow water, interaction with the inhomogeneous ocean bottom is generally more important. In seawater, density fluctuations are generally an order of magnitude smaller than sound-speed variations, and can be neglected.[1] As a result, a large amount of research has addressed scattering by sound-speed variations only, and has been applied to modeling the effects of internal waves.[2–4] When seabed scattering is considered, however, density fluctuations cannot be neglected and are often dominant.[5,6] Scattering from seabed sound-speed and density fluctuations has two main effects; first, energy is stripped from the coherent part of the acoustic field, and second, the scattered energy affects the acoustic field coherence. The theory developed here attempts to capture both effects.

Chernov[1] and Ishimaru[7] have published well-known treatments of propagation through an unbounded random media. Different approaches are appropriate depending on the scale of fluctuations in the medium. If variations in medium properties are small, a perturbation solution can be sought. This work has been extended to study sound incident from a water half-space on a sediment bottom containing random layers. The half-space problem neglects waveguide effects, which is justified for deep water or for high-frequency shallow-water scenarios. Volumetric scattering from within the bottom can be modeled by assuming the scattering sources are uncorrelated uniform spheres.[8,9] Several authors have developed perturbation approaches based on Chernov's work. Ivakin and Lysanov[10] used a plane wave approach which did not include contributions from lateral waves, while Hines[6] used the method of steepest descent to capture lateral as well as refracted wave contributions. Tang[11] developed a self-consistent perturbation theory to model scattering from sound-speed fluctuations in the sediment. Tang was able to calculate a coherent field-reflection coefficient which included loss due to scattering.[12]

More recently, attention has been focused on the role of bottom randomness in influencing propagation in shallow water waveguides. Tang has developed a modal treatment of reverberation due to both sound-speed and density fluctuations.[13] However, this work is based on the Born approximation and does not allow calculation of mean-field scattering loss.

In this paper, we develop a new, self-consistent theory for modeling volume scattering in the ocean. The methodology used is similar to the rough surface scattering approach of Kuperman and Schmidt.[14,15] In the first section, the basic theory for scattering from random sound-speed and density fluctuations in a three-dimensional ocean is presented. Sound-speed and density fluctuations are assumed to be fully correlated. This work allows calculation of the mean-field attenuation due to volume scattering, as well as the spatial statistics of the scattered field.

The approach presented below is a single-scattering theory. Since waveguide propagation is expected to involve multiple scattering events, a single-scatter theory is clearly not exact. However, Voronovich[16] and others[17,18] have argued that the single-scatter approximation is valid as long as the scatterer correlation length is small compared to ray cycle distances associated with propagating modes. In this case, which is typical for many ocean acoustic scenarios, previously scattered energy will be incoherent with both the mean and locally scattered fields when it returns to the inhomogeneous seabed. The scattering process can then be approximated as a series of uncorrelated interactions with the seabed, with single-scattering theory used to calculate secondary source terms for the reverberant field.

This argument is supported by Berman[19] with regard to calculation of the coherent field-reflection coefficient. Berman compared a full multiple-scattering formulation for

[a]Currently at Cambridge Collaborative, Inc., 689 Concord Ave., Cambridge, MA 02138. Electronic mail: btracey@ccinc.com

waveguides with results for a rough interface separating two half-spaces. Some dependence on roughness height was seen, but significant multiple-scattering effects were found only when the roughness correlation length was long compared to ray cycle distances. Because the coherent field-reflection coefficient can be used to calculate scattering loss, Berman's finding relates directly to the validity of the mode attenuations calculated below.

Recently, Berman has developed a multiple-scattering formulation to derive waveguide reverberation.[20] This work may provide a basis for numerically evaluating the single-scattering approximation for scattered field intensity.

The following sections concentrate on scattering of low-frequency sound from random layers in fluid sediment bottoms. First, we model the scattering from a plane wave incident on the ocean bottom, without taking waveguide effects or mean-field attenuation into account. Numerical examples are used to show the effects of sound-speed and density fluctuations over a range of parameter values. For short correlation lengths, the existence of density fluctuations can significantly enhance backscatter. The examples also show that out-of-plane scattering can be important.

Next, propagation of normal modes in a shallow-water waveguide is studied. A perturbation method is used to estimate mean-field normal mode attenuation coefficients due to scattering. Good agreement is demonstrated with mean-field losses calculated by Tang,[12] though results obtained from the modal approach are somewhat sensitive to the modeling of the continuous spectrum.

Finally, the theory developed here can be used to calculate the spatial correlation and cross-modal coherences for the scattered and total fields propagating in the ocean waveguide. A numerical implementation of the volume-scattering theory for a two-dimensional ocean is described elsewhere.[21,22] The close correspondence between the volume-scattering theory and Kuperman and Schmidt's rough-scattering theory facilitates comparison of the different scattering mechanisms.

I. THEORY

The wave equation for inhomogeneous medium has been derived by several authors, including Chernov.[1] Assuming harmonic time dependence, we write the inhomogeneous Helmholtz equation

$$[\nabla^2 + k^2(\mathbf{r},z)]p(\mathbf{r},z) - \frac{\nabla\rho(\mathbf{r},z)}{\rho(\mathbf{r},z)} \cdot \nabla p(\mathbf{r},z) = S_\omega \delta(\mathbf{x}-\mathbf{x}_s), \tag{1}$$

where a point source of strength S_ω located at $x_s=(0,0,z_s)$. We assume that there are small variations in both density and sound speed. In addition, we assume that variations in the sound speed and density are linked. Following Hines,[6] sound speed and density are then written as functions of the bottom *porosity* P.[6] If the background density is constant, we can write

$$c(\mathbf{r},z) = c_0(z) + \frac{\partial c}{\partial P}\,\delta P(\mathbf{r},z),$$

$$\rho(\mathbf{r},z) = \rho_0 + \frac{\partial \rho}{\partial P}\,\delta P(\mathbf{r},z), \tag{2}$$

where δP is the variation in the bottom porosity. Hines gives empirical values of the derivatives to be $\partial\rho/\partial P = -1.440\ \mathrm{g/cm^3}$ and $\partial c/\partial P = -570\ \mathrm{m/s}$. Next, we expand the pressure field in terms of a coherent mean field and an incoherent diffusely scattered field

$$p(\mathbf{r},z) = \langle p(\mathbf{r},z)\rangle + s(\mathbf{r},z). \tag{3}$$

Inserting this expansion in Eq. (1) above and averaging (remembering that sound-speed and density fluctuations are zero mean) gives an equation for the coherent field

$$[\nabla^2 + k_0^2(z)]\langle p(\mathbf{r},z)\rangle - \mu_c(z)\langle \delta P(\mathbf{r},z) s(\mathbf{r},z)\rangle - \mu_\rho \langle \nabla\,\delta P(\mathbf{r},z)\cdot\nabla s(\mathbf{r},z)\rangle = S_\omega \delta(\mathbf{x}-\mathbf{x}_s), \tag{4}$$

where the quantities

$$\mu_c(z) \equiv \frac{2k_0^2(z)\,\partial c/\partial P}{c_0(z)}, \quad \mu_\rho \equiv \frac{1}{\rho_0}\frac{\partial\rho}{\partial P}, \tag{5}$$

have been introduced to simplify the notation.

Subtracting this equation from the full unaveraged Helmholtz equation, we find an expression for the scattered field

$$[\nabla^2 + k_0^2(z)]s(\mathbf{r},z) = \mu_c(z)\,\delta P(\mathbf{r},z)\langle p(\mathbf{r},z)\rangle + \mu_\rho \nabla(\delta P(\mathbf{r},z))\cdot\nabla\langle p(\mathbf{r},z)\rangle. \tag{6}$$

In deriving this equation, we have made a single-scatter approximation by neglecting several terms involving products of the scattered field and the porosity fluctuations. This assumes that the scattered field produced during each scattering event is small. This equation is equivalent to Hines' Eq. (2). As discussed in the Introduction, single-scatter theory can be applied to waveguide propagation under the assumption that seabed inhomogeneity correlation lengths are much shorter than length scales over which scattered energy returns to the seabed (i.e., ray cycle distances).

The first term on the right-hand side above accounts for scattering generated by sound-speed fluctuations, and is monopole-like. The second term, which represents scattering from density fluctuations, will be shown below to enhance backscattering.

Our solution proceeds in a manner analogous to that of Kuperman and Schmidt. First, the equations above are Fourier transformed to yield expressions in the form of the depth-separated wave equation. We then find a solution for the transformed scattered field $\tilde{s}$ in terms of the coherent field. This solution is substituted into the transformed version of Eq. (4) to give a self-consistent equation for the coherent field. This equation takes into account the loss of coherent field energy due to scattering.

We begin by applying the 2-D wave number transform as defined in Ref. 15. Recognizing the right-hand side of Eq. (6) to be a source term distributed over depth, we can write the scattered field as (see Appendix A for details)

$$\tilde{s}(\mathbf{q},z) = -\int\int dz_0\, d\mathbf{k}'\, G_\omega(\mathbf{q},z,z_0)\Bigg[b_1(q,k') \times \widetilde{\delta P}(\mathbf{q}-\mathbf{k}',z)\langle \tilde{p}(\mathbf{k}',z_0)\rangle + \mu_\rho \frac{\partial \widetilde{\delta P}(\mathbf{q}-\mathbf{k}',z_0)}{\partial z_0}\frac{\partial\langle \tilde{p}(\mathbf{k}',z_0)\rangle}{\partial z_0}\Bigg], \tag{7}$$

where

$$b_1(q,k) = \mu_c(z_0) - \mu_\rho(\mathbf{q}-\mathbf{k})\cdot\mathbf{k}. \tag{8}$$

The horizontal derivatives in the density term have become algebraic factors of k and q.

Similarly, we can transform the mean-field equation, giving (see Appendix A)

$$[L(\mathbf{k}) + I(\mathbf{k},z)]\langle \tilde{p}(\mathbf{k},z)\rangle = S_\omega \delta(z-z_s), \tag{9}$$

where the operator

$$L(\mathbf{k}) = \frac{\partial^2}{\partial z^2} + k_0^2(z) - \mathbf{k}^2 \tag{10}$$

is the standard propagation operator for the depth-separated wave equation, and the scattering loss term

$$I(\mathbf{k},z) = -\frac{1}{2\pi}\int d^2\,\mathbf{q}\Bigg[a_1\langle \widetilde{\delta P}(\mathbf{k}-\mathbf{q},z)\tilde{s}(\mathbf{q},z)\rangle + \mu_\rho\Bigg\langle \frac{\partial \widetilde{\delta P}(\mathbf{k}-\mathbf{q},z)}{\partial z}\frac{\partial \tilde{s}(\mathbf{q},z)}{\partial z}\Bigg\rangle\Bigg] \tag{11}$$

describes scattering out of the mean-field wave number k into scattered-field wave numbers q as a function of depth. Equations (7) and (9) are combined to eliminate the scattered-field variable $\tilde{s}$, giving an equation involving only the coherent field $\langle\tilde{p}\rangle$. This substitution results in several second-moment expectations of the porosity fluctuations and their z-derivatives. We model the fluctuation statistics as being described by a correlation function which is separable into horizontal and vertical components

$$\langle \delta P(\mathbf{r},z)\,\delta P(\mathbf{r}+\boldsymbol{\rho},z_0)\rangle = \langle\sigma^2\rangle N(\mathbf{p}) M(z-z_0). \tag{12}$$

This is rewritten in the wave number domain as

$$\langle \widetilde{\delta P}(\mathbf{k},z)\widetilde{\delta P}(\mathbf{q},z_0)\rangle = 2\pi\langle\sigma^2\rangle P_H(\mathbf{q})\,\delta(\mathbf{k}+\mathbf{q})M(z-z_0), \tag{13}$$

where P_H is the power spectrum of horizontal fluctuations. Vertical derivatives of expectations involving δP translate into z-derivatives of M, which can be eliminated from the depth integrals using integration by parts. The detailed calculations are shown in Appendix B. The only restrictions placed on M are that $M(z-z_0)\to 0$ and and $\partial M(z-z_0)/\partial z \to 0$ as the depth separation $z-z_0$ becomes large. These conditions are satisfied by a number of physically reasonable correlation functions, for example Gaussian or decaying exponential forms of $M(z-z_0)$.

After the integrations by parts, the final form of the scattering loss correction term is

$$I(\mathbf{k},z) = \Bigg[F_1(\mathbf{q},\mathbf{k},z_0)\langle\tilde{p}(\mathbf{k},z_0)\rangle + F_2(\mathbf{q},\mathbf{k},z_0)\frac{\partial\langle\tilde{p}(\mathbf{k},z_0)\rangle}{\partial z_0}\Bigg]. \tag{14}$$

The quantities in the correction term are

$$F_1(\mathbf{q},\mathbf{k},z_0) = a_1 a_2 G_\omega(\mathbf{q},z,z_0) + \mu_\rho\Bigg[a_3\frac{\partial^2 G_\omega(\mathbf{q},z,z_0)}{\partial z\,\partial z_0} - a_4\frac{\partial G_\omega(\mathbf{q},z,z_0)}{\partial z}\Bigg], \tag{15}$$

and

$$F_2(\mathbf{q},\mathbf{k},z_0) = \mu_\rho(a_3 - a_1)\frac{\partial G_\omega(\mathbf{q},z,z_0)}{\partial z_0}, \tag{16}$$

where

$$\begin{aligned} a_1 &= \mu_c(z_0) - \mu_\rho(\mathbf{k}-\mathbf{q})\cdot\mathbf{q},\\ a_2 &= \mu_c(z_0) + \mu_\rho(k_0^2 - \mathbf{q}\cdot\mathbf{k}),\\ a_3 &= \mu_c(z_0) + \mu_\rho(2k_0^2 - \mathbf{k}\cdot(\mathbf{k}+\mathbf{q})),\\ a_4 &= \frac{2\mu_\rho k_0^2(z_0) + 3\mu_c(z_0)}{c_0(z_0)}\frac{\partial c_0}{\partial z_0}. \end{aligned} \tag{17}$$

The algebraic terms multiplying the μ_ρ terms in $a_1 - a_3$ result from horizontal and vertical derivatives. All terms including z-derivatives of the pressure field or Green's function also involve only the density fluctuations. These terms result from the spatial derivative term, $\Delta\rho(\mathbf{r},z)/\rho(\mathbf{r},z)$, in the inhomogeneous Helmholtz equation. The term a_4 takes account of any sound-speed gradient in the seabed.

This integro-differential equation is in general difficult to solve. However, experimental studies have shown that the vertical correlation lengths of fluctuations in sediment bottoms are usually quite short. For low frequencies, the vertical correlation length will be much smaller than an acoustic wavelength. It is then reasonable to approximate the vertical correlation function as a delta function[11]

$$M(z-z_0) \approx z_{\mathrm{CL}}\,\delta(z-z_0). \tag{18}$$

This delta function eliminates the depth integral in the mean-field equation. A perturbation solution can be used to estimate mean-field scattering loss, as detailed in Sec. III.

II. PLANE WAVE SCATTERING FROM SEDIMENT BOTTOMS: POWER SPECTRAL DENSITY

As a first application of the theory, we study plane wave scattering from a sediment bottom. A great deal of physical insight can be obtained by looking at the power spectral density $\langle\tilde{s}(\mathbf{q},z)\tilde{s}^*(\mathbf{q},z)\rangle$, the power scattered into each wave number q. This expectation includes cross-terms involving expectations of M and its z-derivatives, which can be simplified using integration by parts as above. The detailed calculations are discussed in Appendix A, with the final result

$$P_{\mathrm{Scat}}(\mathbf{q},z)=\langle \tilde{s}(\mathbf{q},z)\tilde{s}^{*}(\mathbf{q},z)\rangle$$
$$=2\pi\langle\sigma^{2}\rangle\int dz_{0}\int d\mathbf{k}P_{H}(\mathbf{q}-\mathbf{k})$$
$$\times\left|\Delta^{(1)}\frac{\partial G_{\omega}(\mathbf{q},z,z_{0})}{\partial z_{0}}+\Delta^{(2)}G_{\omega}(\mathbf{q},z,z_{0})\right|^{2}, \tag{19}$$

where

$$\Delta^{(1)}(\mathbf{k},z)=-\mu_{\rho}\frac{\partial\langle\tilde{p}(\mathbf{k},z)\rangle}{\partial z}$$
$$\Delta^{(2)}(\mathbf{q},\mathbf{k},z)=a_{2}(\mathbf{q},\mathbf{k},z)\frac{\partial\langle\tilde{p}(\mathbf{k},z)\rangle}{\partial z}. \tag{20}$$

We consider the case of a single plane wave incident on the sediment from the water column and scattering into plane waves in the sediment. As we are mainly concerned with angular distribution of the scattered energy, we will defer calculation of mean-field scattering loss until the next section. Ignoring scattering losses (the Born approximation), the coherent field is replaced by the unperturbed field: $\langle\tilde{p}(\mathbf{k},z)\rangle\approx\tilde{p}_{0}(\mathbf{k},z)$. The incident field in the bottom is then of the form

$$\tilde{p}_{0}(\mathbf{k},z_{0})=T_{12}(k)e^{-ik_{z2}z_{0}}, \tag{21}$$

where $T_{12}(k)$ is the transmission coefficient from the water into the sediment. We choose the Green's function to be the free-space Green's function. Thus, we can only evaluate the scattered field for receivers in the bottom medium. We will evaluate it at $z=0$, the water–sediment interface. The depth-dependent Green's function is given by

$$G_{\omega}(\mathbf{q},z,z_{0})=-\frac{e^{-iq_{z2}|z-z_{0}|}}{4\pi iq_{z2}}. \tag{22}$$

The square root singularity in the Green's function is not physically meaningful and can be removed by changing the variables of integration,[23] so it is not shown in the following plots.

The scattered field is strongly affected by the power spectrum chosen to represent the inhomogeneities. For these calculations, both two-dimensional Gaussian and Goff–Jordan[24] spectra are used

$$P_{\mathrm{Gauss}}(\mathbf{q})=\frac{L_{x}L_{y}}{2}e^{-[(L_{x}q_{x})^{2}+(L_{y}q_{y})^{2}]/4},$$
$$P_{\mathrm{Goff-Jordan}}(\mathbf{q})=\frac{L_{x}L_{y}}{[(L_{x}q_{x})^{2}+(L_{y}q_{y})^{2}+1]^{2}}, \tag{23}$$

where L_x and L_y are the correlation lengths in x and y, respectively. The Goff–Jordan spectrum is more peaked near its maximum and contains much more energy at higher wave numbers. This spectrum has been used in modeling rough-surface scattering,[18] and is chosen to reflect the idea that we expect variations in nature at many length scales. Also, it describes a power-law roll-off at high wave numbers like those measured by Yamamoto.[25]

Figures 1–5 show scattered-field power spectral density (PSD) for several scenarios. The spectra are plotted versus horizontal wave numbers in the x and y directions. A 100-Hz plane wave is assumed to be incident on the bottom along the x-axis ($q_y=0$), at a 10-deg vertical angle. The bottom properties are $\rho=1.9\ \mathrm{g/cm^3}$, $c_b=1650$ m/s, and $\delta c/c_0=0.1$. For this combination of incident angle and bottom type, the incident wave is evanescent in the bottom. Shown on the plot are the sediment wave number k_b (inner circle) and water wave number k_w (outer circle). Wave numbers inside the $|k|=k_b$ circle correspond to the continuous spectrum, wave numbers between the circles correspond to the discrete spectrum, and wave numbers outside the $|k|=k_w$ circle correspond to waves which are evanescent in both the water and sediment.

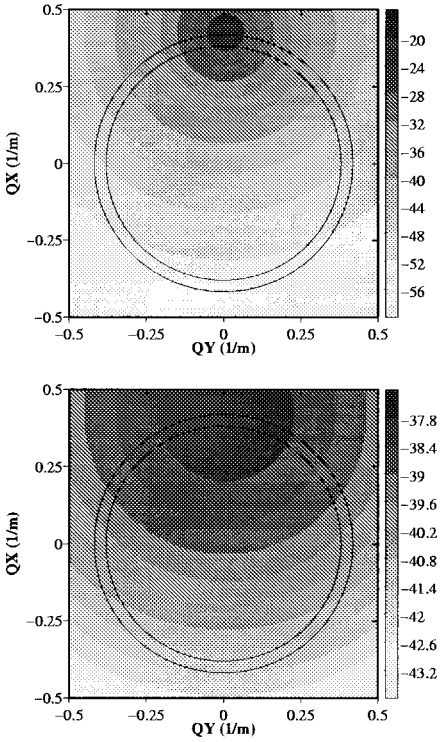

FIG. 1. Plane wave scattering from sound-speed fluctuations only. $f=100$ Hz; Goff–Jordan power spectrum, 10-deg incident wave; correlation lengths of 10 m (upper) and 1 m (lower).

Figures 1 and 2 compare the effect of the choice of power spectrum. Results for correlation lengths of 10 m and 1 m are shown. For these plots, scattering from sound-speed

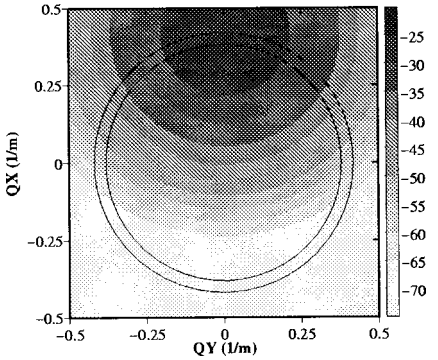

FIG. 2. Plane wave scattering from sound-speed fluctuations. $f=100$ Hz; Gaussian power spectrum, 10-deg incident wave; correlation length is 10 m. Note the Gaussian spectrum gives lower backscattering levels.

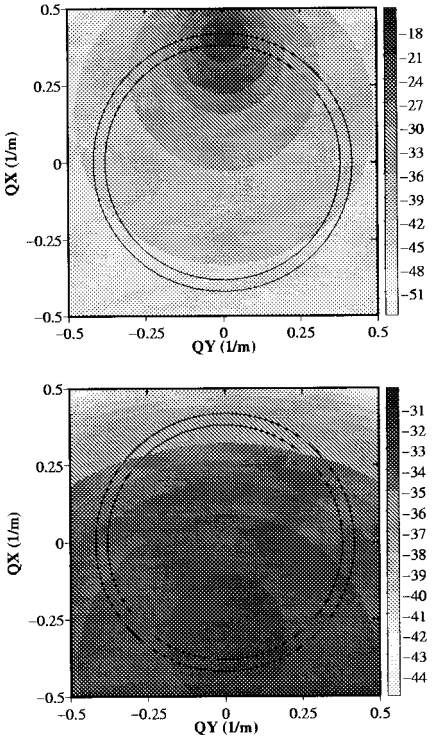

FIG. 3. Plane wave scattering from sound-speed and density fluctuations. $f=100$ Hz; Goff–Jordan power spectrum, 10-deg incident wave; correlation lengths of 10 m (upper) and 1 m (lower). For the shorter correlation length, density fluctuations greatly increase backscatter.

fluctuations alone is included. Comparing the plots for 10-m correlation lengths, the most striking difference is that the backscatter is greatly enhanced with the Goff–Jordan spectrum (Fig. 1) due to the longer tails of the power spectrum. Strong out-of-plane scattering is seen with both spectra, though a peak is observed at angles close to in-plane. In both cases the scattering is basically forward-directed, with the peak in scattered energy centered around the specular direction. Decreasing the correlation length to 1 m gives a much broader distribution of scattered energy. This is expected, since in the limit of small correlation length the inhomogeneities can be thought of as a random distribution of independent point scatterers. Each of these point scatterers radiates isotropically, so the overall scattering pattern is more diffuse. Decreasing the correlation length is also seen to reduce the peak scattered power considerably. This can be understood by remembering that sound will scatter most strongly from objects roughly the size of the wavelength or larger. Since the acoustic wavelength in this case is 16.5 m, most of the sound-speed fluctuations for the 1-m correlation length will have horizontal scales much less than a wavelength.

Figure 3 shows scattering from both sound-speed and density fluctuations in the sediment bottom. For the 10-m correlation length, the scattering intensity levels are only slightly higher than in the case without density fluctuations. Thus, we conclude that, for long horizontal correlation lengths, scattering from sound-speed fluctuations is dominant. When the correlation length is decreased to 1 m, the density scattering is dominant, as seen by comparing Figs. 1 and 3. Most importantly, the maximum is now in the *back-scattered* direction. This backscattering was predicted by Chernov for 1-D scattering, and can be seen in the $\mathbf{q}-\mathbf{k}$ term in Eq. (7), which shows the density-scattering contribution has a null in the forward direction. This preferential scattering in the backward direction can be understood by noting that spatial derivative operators in the density-scattering term have the effect of ''roughening'' the spectrum, emphasizing smaller-scale variability and increasing backscatter.

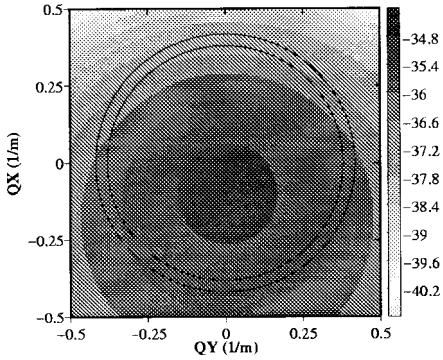

FIG. 4. Plane wave scattering from sound-speed and density fluctuations. $f=100$ Hz; Goff–Jordan power spectrum, 10-deg incident wave; normalized sound-speed and density fluctuations are adjusted to be equal.

The results so far have used Hines' empirically determined values of $\partial c/\partial P$ and $\partial \rho/\partial P$. These values were determined from a limited dataset, and can be expected to vary for different types of sediment bottom. Hines' values predict that the normalized density fluctuations $\delta\rho/\rho_0$ are about twice the normalized sound-speed fluctuations $\delta c/c_0$. In Fig. 4, results are shown in which $\delta\rho/\rho_0$ is adjusted so the normalized sound-speed and density fluctuations are equal. The effect of the density fluctuations is somewhat reduced, but still quite significant.

We can also study the effects of anisotropy in seabed property fluctuations. Figure 5 shows scattering of plane waves on a bottom with a correlation length of 2 m in x and 10 m in y. Increasing the correlation length in y gives a power spectrum with much less width in q_y. In Fig. 5 we let a plane wave be incident on the bottom at a vertical angle of 10 deg, and horizontal angles of 0 (along the x-axis), 45 deg, and 90 deg (along the y-axis). From observing the plots, we see that the anisotropy causes the scattered field to be skewed away from the incident angle for incident angles not aligned with the principal axes of the inhomogeneities. The anisotropy causes increased scattering into the continuous spectrum for the 0-deg incident wave, vs increased out-of-plane scattering for the 90-deg incident wave.

III. MODAL SCATTERING FROM RANDOM SEDIMENT BOTTOMS

For low-frequency shallow water propagation, the acoustic field is often well described as a sum of a reasonably small number of normal modes. This leads us to specialize the theory developed above to consider scattering of a modal sound field from inhomogeneities in fluid sediment bottoms. In doing so, we will make a number of simplifying assumptions. The most useful of these, discussed above, is that the vertical correlation function can be approximated as

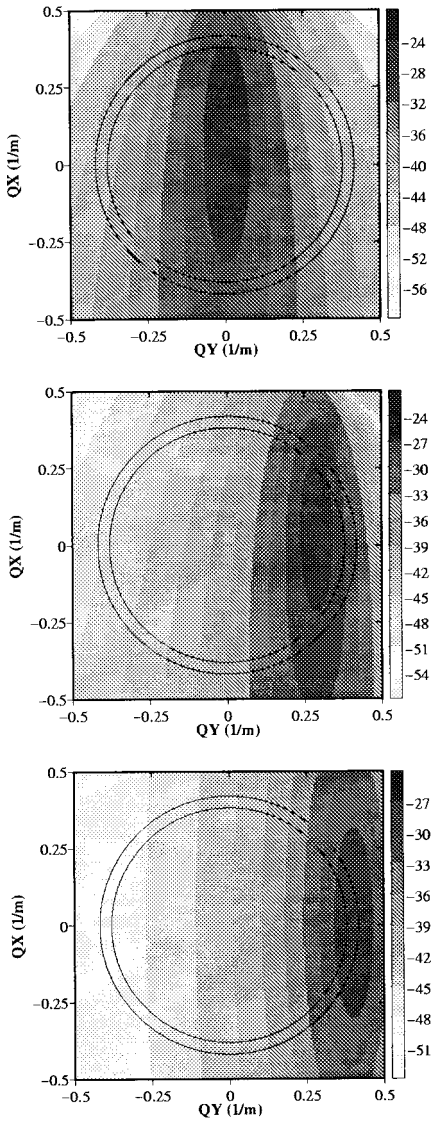

FIG. 5. Plane wave scattering from anisotropic sound-speed and density fluctuations, for incident angles of (from top) 0, 45, and 90 deg. $f = 100$ Hz; Goff–Jordan power spectrum; CL$x = 2$ m, CL$y = 10$ m.

a delta function. The second major simplification made is that the sound speed is constant in the layer where volume fluctuations are present. This assumption is limiting, but allows us to examine the basic scattering physics. For isovelocity layers, the field can be written in terms of up- and down-going plane waves, so depth integrals in the scattered-field expressions can be treated analytically. Depth integrals over the incident field modes and their derivatives must otherwise be performed numerically, making the calculations much slower and less accurate.

KRAKEN[26] or any other normal mode code can used to find the mode shapes and eigenvalues for the waveguide. The continuous spectrum contribution is included by introducing a false bottom deep in the sediment. The modal problem is then converted to a proper Sturm–Liouville problem and all modes are proper modes. Since there are both up- and down-going plane waves in the scattering layer, we write the mode shape as

$$\psi_n(z) = \begin{cases} \zeta_n(z), & z < z_1, \\ A_n e^{-ik_{zn}(z-z_1)} + B_n e^{ik_{zn}(z-z_1)}, & z > z_1, \end{cases} \tag{24}$$

where $\zeta_n(z)$ are the mode shapes found by the normal mode program and z_1 is the top of the volume-scattering layer. The plane wave coefficients A_n and B_n are found from the boundary conditions at the interface z_1, and sediment attenuation is included by introducing an imaginary part of the bottom wave number (Ref. 23, Chap. 2).

A. Mode attenuation coefficients

In this section, the mean-field equation is solved to find mean-field modal attenuations. This requires evaluating the scattering-loss correction term $I(k,z)$ from Eq. (9). The correction term is an $O(\sigma^2)$ perturbation to the mean field. Since the scattering theory retains terms only up to $O(\sigma^2)$, it is consistent to use the unperturbed eigenvalues and eigenfunctions when calculating $I(\mathbf{k},z)$; i.e., $I(\mathbf{k},z) \approx I(\mathbf{k}_0,z)$. This argument was made by Kuperman[27] in studying rough-surface scattering.

The scattering-loss correction contains terms proportional to both the mean field and its depth derivative [see Eq. (14)]. If we calculate attenuations for the propagating modes of the waveguide only, we can take advantage of the fact that these modes are exponentially decaying in the bottom to relate these terms by

$$\frac{\partial \langle \tilde{p}(\mathbf{k},z) \rangle}{\partial z} = -\alpha_b \langle \tilde{p}(\mathbf{k},z) \rangle, \tag{25}$$

where $\alpha_b = \sqrt{\mathbf{k}^2 - k_b^2}$. This lets us simplify the correction term and write the homogeneous mean-field equation in the form

$$[L(\mathbf{k}) + \langle \sigma^2 \rangle f(\mathbf{k},z)] \langle \tilde{p}(\mathbf{k},z) \rangle = 0, \tag{26}$$

where $f(\mathbf{k},z)$ is a combination of the F_1 and F_2 terms from Eq. (14).

We next substitute the modal forms of the Green's function (as a sum over modes m) into the mean-field equation, and switch to polar coordinates: $\int d^2\,\mathbf{q} = \int\int q\,dq\,d\theta$. Integrating over q exposes poles at $q = q_m$, leaving the integration over θ. Physically, this means that the scattered field will travel in the modes of the waveguide, but can be scattered into any horizontal angle. The correction term f becomes

$$\begin{aligned} f(\mathbf{k},z) = \frac{iz_{\mathrm{CL}}}{2\rho(z)} \int d\theta \sum_{m=1}^{M} P_H(\mathbf{q}_m - \mathbf{k}) [a_1 a_2 \psi_m^2(z) \\ + \mu_\rho a_3 (\psi_m'(z))^2 - \mu_\rho (a_4 - \alpha_b(z)(a_1 - a_2 \\ + \mu_\rho [q_m^2 - k_0^2(z)])) \psi_m(z) \psi_m'(z)]. \end{aligned} \tag{27}$$

Here, we have left implicit the dependence of the a_i terms

$$a_i = a_i(\mathbf{q}_m, \mathbf{k}, z), \tag{28}$$

where $\mathbf{q} = (q_m \cos\theta, q_m \sin\theta)$.

This equation can be rewritten in the form of an eigenvalue perturbation problem, giving

$$\left[\frac{\partial^2}{\partial z^2} + k_0^2(z) \right] \psi_n = k_n^2 \psi_n - \langle \sigma^2 \rangle f(\mathbf{k}_n, z) \psi_n. \tag{29}$$

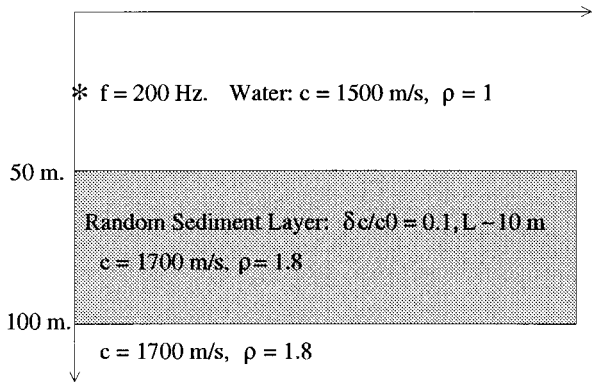

FIG. 6. Scenario for comparison with Tang's results. $f=200$ Hz; Gaussian spectrum, 10-m correlation length, $\delta c/c_0=0.1$.

The new eigenvalue can then be found using perturbation theory, as described by Bender and Orzag.[28] Appendix B shows that the first-order correction for the eigenvalue is

$$\Delta k_n=\frac{\langle\sigma^2\rangle}{2k_{n0}}\int_0^D\frac{f(\mathbf{k}_{n_0},z)\psi_n^2(z)}{\rho(z)}dz. \tag{30}$$

The imaginary part of Δk_n is the mode attenuation coefficient.

To validate our approach, we compare our method to results obtained by Tang[11] for a bottom containing sound-speed fluctuations only. Tang's code was used to calculate mean-field plane wave reflection coefficients for the sediment bottom. These reflection coefficients were used as a boundary condition for the normal mode code KRAKEN, which calculated the modified eigenvalues. The resulting change in the mode attenuation was taken to be Tang's prediction for scattering loss.

KRAKEN was then used to find the eigenvalues and mode shapes for the unperturbed scenario. These were used to find the mode attenuations from Eq. (30).

A simple scenario, shown in Fig. 6, was used for comparison. A 50-m-deep isovelocity water layer overlays a sediment half-space, the upper 50 m of which contains sound-speed inhomogeneities. The inhomogeneities are assumed to have a 2-D isotropic Gaussian correlation function in the horizontal and to be delta-correlated in the vertical. Attenuation in the water and sediment is neglected, so any loss is purely due to scattering.

Figure 7 shows the plane wave reflection coefficient for correlation function parameters which are used by Tang: $\delta c_{\rm rms}/c_0=0.1$, horizontal correlation length $l_0=10$ m, and vertical correlation length $z_{\rm CL}=1$ m.

The modal results are compared with Tang's attenuation coefficients in Fig. 8. Attenuation coefficients obtained using the modal approach are in reasonably good agreement with Tang's results, but are sensitive to the treatment of the continuous spectrum. However, the otherwise good agreement suggests that the approaches are compatible in describing the scattering physics.

Figure 8 shows modal attenuation coefficients for $f=200$ Hz, calculated from Tang's results and from the modal

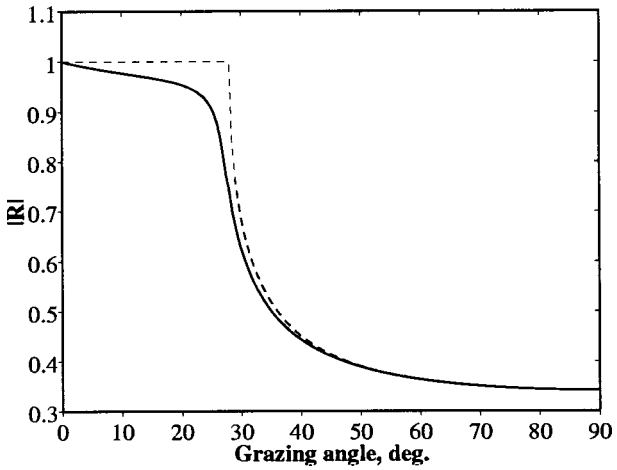

FIG. 7. Reflection coefficients for scenario. Dashed line is for nonrandom bottom; solid line is for bottom with random layer.

approach described above. When only scattering into proper modes is allowed, the modal calculation is seen to significantly underestimate the actual attenuation.

Scattering into the continuous spectrum is then approximated numerically by introducing a false bottom at 400-m depth (note we can allow a false bottom without any bottom attenuation only because we are interested here in scattering *into* the continuous spectrum; when calculating statistics of the scattered field, we must always include bottom attenuation so the continuous spectrum modes will decay quickly with range). When these extra modes are included, the agreement from the two methods is greatly improved. However, attenuations calculated using the modal approach are sensitive to the number of continuous spectrum modes included. As the number of modes included is increased, the results converge to the attenuations shown in Fig. 8, which includes 111 false-bottom modes in addition to the 6 proper modes. A calculation which includes 41 false-bottom modes shows nearly exact agreement with Tang's results for modes 1–4, but underestimates attenuation for modes 5 and 6.

This sensitivity is not surprising, as the normal mode

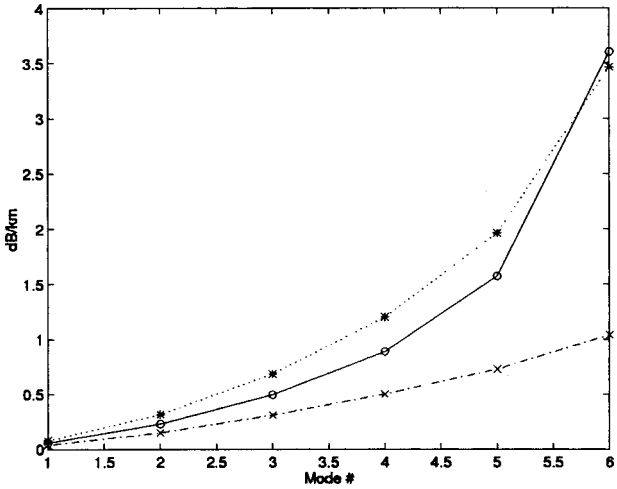

FIG. 8. Comparison with Tang's results. Open circles shows results from Tang; asterisk shows modal solution including continuous spectrum modes; "×" shows modal solution, proper modes only.

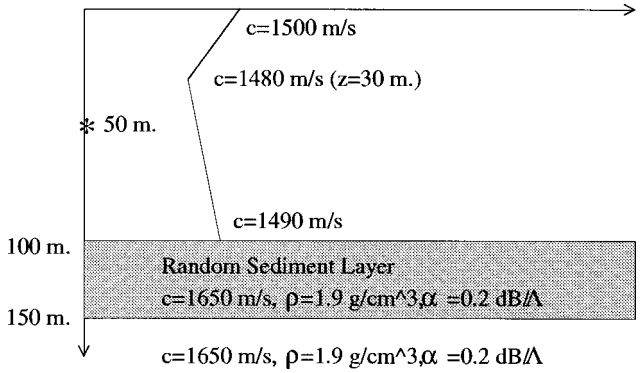

FIG. 9. Shallow water scattering scenario.

approach is known to have difficulty in modeling the continuous spectrum. The two main conclusions to be drawn from Fig. 8 are: first, that the current approach appears to agree with earlier work, and second, that scattering losses can be estimated fairly accurately with a modal approach. In many practical cases, uncertainty in environmental parameters will be larger than errors introduced by modeling of continuous spectrum modes.

Next, the fluid bottom, shallow water waveguide shown in Fig. 9 is considered. Both sound-speed and density fluctuations are included. For notational convenience, we define a parameter σ, which is set equal to the normalized sound-speed fluctuations $\delta c/c_0$. For a given σ, the density fluctuations are found from the relationship between density and sound-speed fluctuations given by Hines' constants.

We again examine horizontal correlation lengths of 1 and 10 m. The random scattering layer is assumed to be between 100- and 150-m depth. For the 10-m correlation length, seen in the upper plot of Fig. 10, including density scattering causes only a slight increase in mode attenuation. However, density fluctuations are the predominant cause of loss for the shorter 1-m correlation length case, shown in the lower plot of Fig. 10. This agrees with the trends seen above for plane wave scattering. The full scattering loss with the 1-m correlation length is of roughly the same order of magnitude as the loss caused by a bottom attenuation of 0.1 dB/λ. Whether or not attenuation due to volume scattering is a significant attenuation mechanism will depend on the environment considered. However, it has been demonstrated numerically[21] that the coherent field loss can significantly affect the correlation statistics of the total field.

IV. CONCLUSION

In this paper, a new self-consistent theory describing scattering from volume fluctuations in the ocean has been developed which includes scattering from both sound-speed and density fluctuations and allows calculation of coherent field attenuation due to scattering. Previous modeling including both sound-speed and density fluctuations has been based on the Born approximation, and does not give coherent field-scattering loss. The effects of including density fluctuations in a 3-D ocean were examined. When the horizontal correlation length of scatterers is small, scattering from density fluctuations significantly changes the backscattered energy.

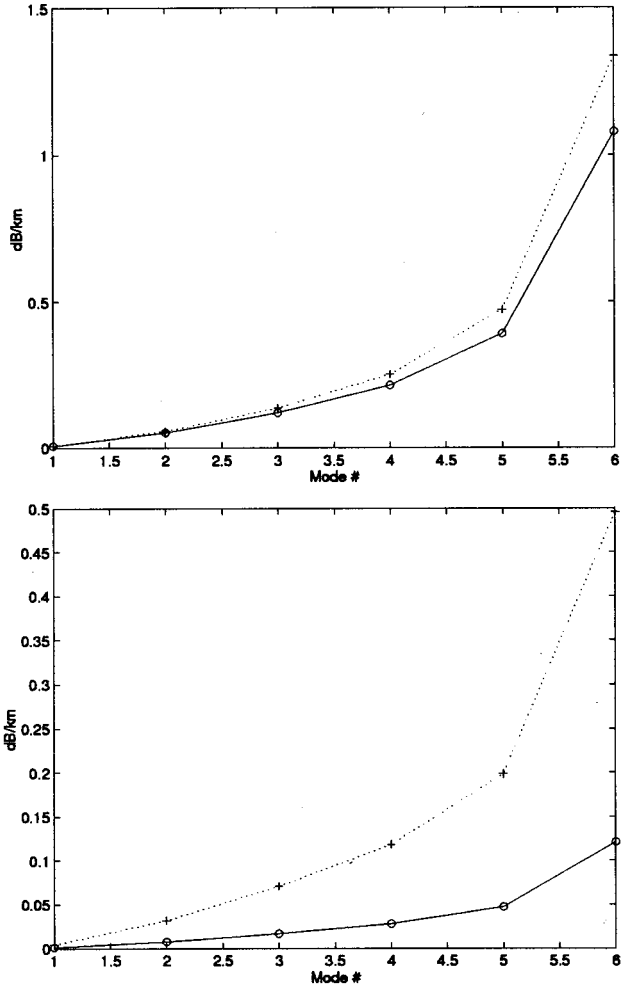

FIG. 10. Mode attenuations for shallow water example. $f=100$ Hz; Goff–Jordan spectrum, $\sigma=0.1$. Solid line includes effect of both sound-speed and density fluctuations, dotted line includes sound-speed fluctuations only. Correlation lengths of 10 m (upper plot) and 1 m (lower plot) are assumed.

The effects of out-of-plane scattering and anisotropic fluctuation statistics are also shown to be important. The theory was extended to find modal attenuations due to scattering, showing agreement with previous work which included sound-speed fluctuations only. For scenarios involving both sound-speed and density fluctuations, modal scattering losses can be comparable in magnitude to the effects of bottom attenuation.

ACKNOWLEDGMENTS

The authors gratefully acknowledge the support of the Office of Naval Research, under Contracts Nos. N00014-92-J-1282 and N00014-95-1-0307. Suggestions by Dr. Dajun Tang and Dr. Dan Li were very helpful.

APPENDIX A: SCATTERING INTEGRALS AND MEAN FIELD EQUATION

In this Appendix, the details of several calculations referred to above are shown. Before beginning we state several relationships which will be of use. From the definition of the wave number transform,

$$\delta P(\mathbf{r},z)=\frac{1}{2\pi}\int_{-\infty}^{\infty}d^2\,\mathbf{k}\widetilde{\delta P}(\mathbf{k},z)e^{-i\mathbf{k}\cdot\mathbf{r}}, \tag{A1}$$

$$\langle p(\mathbf{r},z)\rangle=\frac{1}{2\pi}\int_{-\infty}^{\infty}d^2\,\mathbf{k}\langle\tilde{p}(\mathbf{k},z)\rangle e^{-i\mathbf{k}\cdot\mathbf{r}}, \tag{A2}$$

$$s(\mathbf{r},z)=\frac{1}{2\pi}\int_{-\infty}^{\infty}d^2\,\mathbf{k}\tilde{s}(\mathbf{k},z)e^{-i\mathbf{k}\cdot\mathbf{z}}. \tag{A3}$$

Horizontal derivatives are transformed into algebraic factors; for example

$$\frac{\partial\delta P(\mathbf{r},z)}{\partial\mathbf{r}}=\frac{1}{2\pi}\int_{-\infty}^{\infty}d^2\,\mathbf{k}(-i\mathbf{k})\delta\tilde{P}(\mathbf{k},z)e^{-i\mathbf{k}\cdot\mathbf{r}}. \tag{A4}$$

We use also the following property of the delta function:

$$\frac{1}{(2\pi)^2}\int_{-\infty}^{\infty}d^2\,\mathbf{r}e^{i\mathbf{k}\cdot\mathbf{r}}=\delta(\mathbf{k}). \tag{A5}$$

First, we evaluate the wave number transform of the scattered-field equation. From the results in Sec. I, the transformed scattered field is given by

$$L(\mathbf{q})\tilde{s}(\mathbf{q},z)=\frac{1}{2\pi}\int d^2\,\mathbf{r}e^{i\mathbf{q}\cdot\mathbf{r}}[\mu_c(z)\delta P(\mathbf{r},z)\langle p(\mathbf{r},z)\rangle + \mu_\rho\nabla\delta P(\mathbf{r},z)\cdot\langle p(\mathbf{r},z)\rangle]. \tag{A6}$$

The work to be done is in evaluating the right-hand side (rhs). We begin by looking at the simpler first term, which involves only μ_c. Inserting the appropriate definitions from above gives

$$\text{rhs1}=\frac{\mu_c(z)}{(2\pi)^3}\int\int\int d^2\,\mathbf{k}_1d^2\,\mathbf{k}_2d^2\,\mathbf{r}\delta\tilde{P}(\mathbf{k}_1,z)\times\langle\tilde{p}(\mathbf{k}_2,z)\rangle e^{i[\mathbf{q}-(\mathbf{k}_1+\mathbf{k}_2)]\mathbf{r}}. \tag{A7}$$

Using the delta function property and integrating over $\mathbf{r}$

$$\text{rhs1}=\frac{1}{2\pi}\int\int d^2\,\mathbf{k}_1d^2\mathbf{k}_2\widetilde{\delta P}(\mathbf{k}_1,z)\langle\tilde{p}(\mathbf{k}_2,z)\rangle\times\delta[\mathbf{q}-(\mathbf{k}_1+\mathbf{k}_2)]. \tag{A8}$$

The delta function pulls out $\mathbf{k}_1=\mathbf{q}-\mathbf{k}_2$. Renaming $\mathbf{k}_2\equiv\mathbf{k}'$, we have

$$\text{rhs1}=\frac{\mu_c(z)}{2\pi}\int d^2\,\mathbf{k}'\,\delta\tilde{P}(\mathbf{q}-\mathbf{k}',z)\langle\tilde{p}(\mathbf{k}',z)\rangle. \tag{A9}$$

We next examine the second term, which involves spatial derivatives of $\rho(\mathbf{r},z)$. The derivative terms can be expanded into separate horizontal and vertical derivatives. Rewriting in terms of the transformed variables and integrating over $\mathbf{r}$ and $\mathbf{k}_1$ as above gives

$$\text{rhs2}=\frac{-\mu_\rho}{2\pi}\int d^2\,\mathbf{k}'\left[(\mathbf{q}-\mathbf{k}')\cdot\mathbf{k}'\widetilde{\delta P}(\mathbf{q}-\mathbf{k}',z)\times\langle\tilde{p}(\mathbf{k}',z)\rangle-\frac{\partial\widetilde{\delta P}(\mathbf{q}-\mathbf{k}')}{\partial z}\frac{\partial\langle\tilde{p}(\mathbf{k}',z)\rangle}{\partial z}\right]. \tag{A10}$$

Adding these results together gives the combined rhs for the scattered-field equation shown in Eq. (7).

The second result shown is the transformation of the mean-field equation, Eq. (4). Again, we break the equation into two terms, and look at the simpler one, multiplying μ_c first. This term is

$$I1=-\frac{\mu_c(z)}{2\pi}\int_{-\infty}^{\infty}\langle\delta P(\mathbf{r},z)s(\mathbf{r},z)\rangle e^{i\mathbf{k}\cdot\mathbf{z}}d^2\,\mathbf{r}. \tag{A11}$$

The calculation begins by substituting in the expressions for $s(\mathbf{r},z)$ and $\delta P(\mathbf{r},z)$

$$I1=-\frac{\mu_c(z)}{(2\pi)^3}\int\int\int d^2\,\mathbf{r}d^2\,\mathbf{k}_1d^2\,\mathbf{q}\times\langle\delta\tilde{P}(\mathbf{k}_1,z)\tilde{s}(\mathbf{q},z)\rangle e^{i(\mathbf{k}-(\mathbf{k}_1+\mathbf{q}))\mathbf{r}}d^2\,\mathbf{r}. \tag{A12}$$

Integrating over $\mathbf{r}$ again gives a delta function, which is satisfied when $\mathbf{k}_1=\mathbf{k}-\mathbf{q}$. This gives the result

$$I1=-\frac{\mu_c(z)}{2\pi}\int d\mathbf{q}\langle\delta\tilde{P}(\mathbf{k}-\mathbf{q},z)\tilde{s}(\mathbf{q},z)\rangle. \tag{A13}$$

Next, we look at the remaining terms, given by

$$I2=-\frac{\mu_\rho}{2\pi}\int d^2\,\mathbf{r}\left\langle\frac{\partial\delta P(\mathbf{r},z)}{\partial\mathbf{r}}\cdot\frac{\partial s(\mathbf{r},z)}{\partial\mathbf{r}}\right\rangle e^{i\mathbf{k}\cdot\mathbf{r}} - \frac{\mu_\rho}{2\pi}\int d^2\,\mathbf{r}\left\langle\frac{\partial\delta P(\mathbf{r},z)}{\partial z}\cdot\frac{\partial s(\mathbf{r},z)}{\partial z}\right\rangle e^{i\mathbf{k}\cdot\mathbf{r}}. \tag{A14}$$

Carrying out substitutions and integrations exactly as done above gives the result

$$I2=-\frac{\mu_\rho}{2\pi}\int d^2\,\mathbf{q}\left\{-(\mathbf{k}-\mathbf{q})\cdot\mathbf{q}\langle\widetilde{\delta P}(\mathbf{k}-\mathbf{q},z)\tilde{s}(\mathbf{q},z)\rangle + \left\langle\frac{\partial\widetilde{\delta P}(\mathbf{k}-\mathbf{q})}{\partial z}\frac{\partial\langle\mathbf{p}(\mathbf{q},z)\rangle}{\partial z}\right\rangle\right\}. \tag{A15}$$

These two terms are added to give the intermediate result shown in Eq. (11).

We proceed by evaluating the expectation terms above. This calculation is straightforward but long, so we will not show all details here. We first look at the first expectation in Eq. (A13)

$$E_1=\langle\delta\tilde{P}(\mathbf{k}-\mathbf{q},z)\tilde{s}(\mathbf{q},z)\rangle. \tag{A16}$$

Substituting in the expression for $\tilde{s}(q,z)$ from Eq. (7) gives one term involving a second-moment expectation of $\tilde{\delta}\tilde{P}$ and another term involving an expectation of $\tilde{\delta}\tilde{P}$ with its vertical derivative. From the definition of the power spectrum, vertical derivatives of porosity translate into derivatives of the vertical correlation function M. Assuming that the vertical correlation length $z_{\mathrm{CL}}\gg\lambda$ [Eq. (18)] lets us approximate M with a delta function. The first term resulting from Eq. (A16) gives

$$E_{11}=-2\pi\langle\sigma^2\rangle z_{\mathrm{CL}}P_H(\mathbf{q}-\mathbf{k})G_\omega(\mathbf{q},z,z_0)b1(\mathbf{q},\mathbf{k},z)\times\langle\tilde{p}(\mathbf{k},z)\rangle. \tag{A17}$$

The second integral, rewritten

$$E_{12} = -2\pi\langle\sigma^2\rangle P_H(\mathbf{q}-\mathbf{k}) \int z_0\, G_\omega(\mathbf{q},z,z_0) \times \frac{\partial M(z-z_0)}{\partial z_0}\, \frac{\partial\langle\tilde{p}(\mathbf{k},z_0)\rangle}{\partial z_0}, \tag{A18}$$

can be found using integration by parts, following Chernov.[1] Dropping the constants for a moment, we have

$$E_{12} \sim -G_\omega \frac{\partial\langle\tilde{p}\rangle}{\partial z_0} M\Big|_{-\infty}^{\infty} + \int dz_0\, M(z-z_0) \times \left[G_\omega(\mathbf{q},z,z_0)\, \frac{\partial^2\langle\tilde{p}(\mathbf{k},z_0)\rangle}{\partial z_0^2} + \frac{\partial G_\omega(\mathbf{q},z,z_0)}{\partial z_0}\, \frac{\partial\langle\tilde{p}(\mathbf{k},z_0)\rangle}{\partial z_0} \right]. \tag{A19}$$

The first term drops out as $M \to 0$ for large $(z-z_0)$, and Eq. (18) is used to eliminate the depth integral. The second derivative of $\langle\tilde{p}(\mathbf{k},z)\rangle$ is simplified using the Helmholtz equation. Finally, E_1 is found to be

$$E_1 = -2\pi z_{\mathrm{CL}} P_H(\mathbf{q}-\mathbf{k}) \left\{ a_2 G_\omega(\mathbf{q},z,z)\langle\tilde{p}(\mathbf{k},z_0)\rangle - \mu_\rho \frac{\partial G_\omega(\mathbf{q},z,z_0)}{\partial z_0}\Big|_z \frac{\partial\langle\tilde{p}(\mathbf{k},z_0)\rangle}{\partial z_0}\Big|_z \right\}, \tag{A20}$$

where a_2 is as defined in Sec. III A.

The calculation for the second expectation,

$$E_2 = \left\langle \frac{\partial\widetilde{\delta P}(\mathbf{k}-\mathbf{q},z)}{\partial z}\, \frac{\partial\tilde{s}(\mathbf{q},z)}{\partial z} \right\rangle \tag{A21}$$

is similar but more complicated. Substituting in the scattered-field expression again gives two expectations, one of which involves $\partial M(z-z_0)/\partial z$ and the other of which involves $\partial^2 M(z-z_0)/\partial z^2$. Using a change of variables argument, it is easy to show that $\partial M/\partial z = -\partial M/\partial z_0$, giving two integrals which involve derivatives with respect to z_0. We again use integration by parts, using the assumption that $\partial M(z-z_0)/\partial z_0 \to 0$ as $z-z_0$ becomes large to simplify the integral involving $\partial^2 M/\partial {z_0}^2$. Full details of the calculation are found in Ref. 21. Finally, E_1 and E_2 are combined to give the self-consistent equation for the mean field quoted in Eq. (14).

The power-spectral density, defined as $\langle\tilde{s}(\mathbf{q},z)\tilde{s}^*(\mathbf{q},z)\rangle$, measures the scattered energy in wave number $\mathbf{q}$ at depth z. The calculation involves cross-expectations of terms involving δP with terms involving $\partial\delta P/\partial z$, as seen from Eq. (7). These expectations are found using the definition of the power spectrum, Eq. (13), and integration by parts. The details of the calculations are very similar to those shown in the Appendix above and involve the same assumptions about the vertical correlation function M. The delta function resulting from the power spectrum is of the form $\delta(\mathbf{q}-\mathbf{k}_1-\mathbf{q}+\mathbf{k}_2)$, requiring $\mathbf{k}_1 = \mathbf{k}_2$. The resulting terms can be simplified through symmetry, giving the power-spectral density shown in Sec. II.

APPENDIX B: PERTURBATION THEORY FOR EIGENVALUE CORRECTION

Consider the form of the eigenvalue problem above:

$$\left[\frac{\partial^2}{\partial z^2} + k_0^2(z)\right]\psi_n = k_n^2\psi_n - \langle\sigma^2\rangle f(\mathbf{k}_{n_0},z)\,\psi_n. \tag{B1}$$

As this is the equation for the mean field, all quantities above are averaged, though this is not shown explicitly. The equation can be rewritten in the form

$$H\psi_n = E_n\psi_n - \langle\sigma^2\rangle f(\mathbf{k}_{n_0},z)\,\psi_n. \tag{B2}$$

Expanding the perturbed quantities to second order,

$$\begin{aligned} \psi_n &= \psi_n^{(0)} + \sigma\psi_n^{(1)} + \sigma^2\psi_n^{(2)} + \cdots, \\ E_n &= E_n^{(0)} + \sigma E_n^{(1)} + \sigma^2 E_n^{(2)} + \cdots. \end{aligned} \tag{B3}$$

Since we are interested in calculating the mean field, we average the equations above. Since σ is zero-mean, we find

$$\begin{aligned} \langle\psi_n\rangle &= \psi_n^{(0)} + \langle\sigma^2\rangle\psi_n^{(2)} + \cdots, \\ \langle E_n\rangle &= E_n^{(0)} + \langle\sigma^2\rangle E_n^{(2)} + \cdots, \end{aligned} \tag{B4}$$

where all quantities are averaged even if not explicitly written so. Substituting these above and equating terms of like order gives, for the first-order equation,

$$H^{(0)}\psi_n^{(0)} = E_n^{(0)}\psi_n^{(0)}. \tag{B5}$$

This is just the unperturbed equation. The $O(\sigma)$ terms are zero, by inspection. Finally, the second-order equation is

$$H^{(0)}\psi_n^{(2)} = E_n^{(0)}\psi_n^{(2)} + E_n^{(2)}\psi_n^{(0)} - \langle\sigma^2\rangle f(\mathbf{k}_{n_0},z)\,\psi_n^{(0)}. \tag{B6}$$

The first two terms are eliminated using the first-order solution. Operating on the remaining terms with

$$\int \frac{\psi_n^{(0)}}{\rho(z)}(\cdot)\,dz, \tag{B7}$$

and using the normalization condition, gives the result

$$E_n^{(2)} = \langle\sigma^2\rangle \int \frac{(\psi_n^{(0)})^2 f(\mathbf{k}_{n_0},z)}{\rho(z)}\,dz. \tag{B8}$$

We relate this to the eigenvalue perturbation Δk_n by noting that

$$k_n^2 = (k_{n0} + \Delta k_n)^2 = k_{n0}^2 + 2\Delta k_n k_{n0} + O(\sigma^4) + \cdots. \tag{B9}$$

Then, the final expression, quoted in Sec. III A, is

$$\Delta k_n = \frac{1}{2k_{n0}} E_n^{(2)} = \frac{\langle\sigma^2\rangle}{2k_{n0}} \int_0^D \frac{f(\mathbf{k}_{n_0},z)\,\psi_n^2(z)}{\rho(z)}\,dz. \tag{B10}$$

[1] L. A. Chernov, *Wave Propagation in a Random Medium* (McGraw-Hill, New York, 1960).

[2] L. B. Dozier and F. D. Tappert, ''Statistics of normal mode amplitudes in a random ocean: Theory,'' J. Acoust. Soc. Am. **63**, 352–365 (1977).

[3] Y. Desaubies, ''On the scattering of sound by internal waves in the ocean,'' J. Acoust. Soc. Am. **64**, 1460–1468 (1978).

[4] H. Essen, F. Schirmer, and S. Sirkes, ''Acoustic remote sensing of internal waves in shallow water,'' Int. J. Remote Sens. **4**(1), 33–47 (1983).

[5] T. Yamamoto, ''Acoustic scattering in the ocean from velocity and density fluctuations in the sediments,'' J. Acoust. Soc. Am. **99**, 866–879 (1996).

[6] P. Hines, ''Theoretical model of acoustic backscatter from a smooth seabed,'' J. Acoust. Soc. Am. **88**, 324–334 (1990).
[7] A. Ishimaru, *Wave Propagation and Scattering in Random Media* (Academic, New York, 1978).
[8] J. H. Stockhausen, ''Scattering from the volume of an inhomogeneous halfspace,'' NRE Report, 63/9 (1963).
[9] D. Jackson, D. Winebrenner, and A. Ishimaru, ''Application of the composite roughness model to high-frequency bottom backscattering,'' J. Acoust. Soc. Am. **79**, 1410–1422 (1986).
[10] A. N. Ivakin and Y. P. Lysanov, ''Theory of underwater sound scattering by volume inhomogeneities of the bottom,'' Sov. Phys. Acoust. **27**(1), 61–64 (1981).
[11] D. Tang, ''Acoustic Wave Scattering from a Random Ocean Bottom,'' Ph.D. thesis, Massachusetts Institute of Technology and Woods Hole Oceanographic Institute, June 1991.
[12] D. Tang and G. V. Frisk, ''Plane-wave reflection from a random fluid half-space,'' J. Acoust. Soc. Am. **90**, 2751–2756 (1991).
[13] D. Tang, ''Shallow water reverberation due to sediment volume inhomogeneities,'' J. Acoust. Soc. Am. **98**(A), 2988 (1995).
[14] W. A. Kuperman and H. Schmidt, ''Rough surface elastic wave scattering in a horizontally stratified ocean,'' J. Acoust. Soc. Am. **79**, 1767–1777 (1986).
[15] W. A. Kuperman and H. Schmidt, ''Self-consistent perturbation approach to rough surface scattering in stratified elastic media,'' J. Acoust. Soc. Am. **86**, 1511–1522 (1989).
[16] A. G. Voronovich, ''Approximation of uncorrelated reflections in the problem of sound propagation in a waveguide with a statistically rough boundary,'' Sov. Phys. Acoust. **33**(1), 11–17 (1987).
[17] H. Schmidt and W. A. Kuperman, ''Spectral representations of rough interface reverberation in stratified ocean waveguides,'' J. Acoust. Soc. Am. **97**, 2199–2209 (1995).
[18] K. D. LePage and H. Schmidt, ''Modeling of low frequency transmission loss in the central Arctic,'' J. Acoust. Soc. Am. **96**, 1783–1795 (1994).
[19] D. H. Berman, ''Computing effective reflection coefficients in layered media,'' J. Acoust. Soc. Am. **101**, 741–748 (1997).
[20] D. H. Berman, ''Reverberation in waveguides with rough surfaces,'' J. Acoust. Soc. Am. **105**, 672–686 (1999).
[21] B. Tracey, ''An integrated modal approach to surface and volume scattering in ocean acoustic waveguides,'' Ph.D. thesis, Massachusetts Institute of Technology and Woods Hole Oceanographic Institution, January 1995.
[22] B. Tracey and H. Schmidt, ''Seismo-acoustic field statistics in shallow water,'' IEEE J. Ocean Eng. **22**(2), 317–331 (1997).
[23] F. B. Jensen, W. A. Kuperman, M. B. Porter, and H. Schmidt, *Computational Ocean Acoustics* (American Institute of Physics, Woodbury, NY, 1994).
[24] J. Goff and T. Jordan, ''Stochastic modeling of seafloor morphology: Inversion of sea beam data for second order statistics,'' J. Geophys. Res. **93**, 13589–13608 (1993).
[25] T. Yamamoto, ''Velocity variabilities and other physical properties of marine sediments measured by crosswell acoustic tomography,'' J. Acoust. Soc. Am. **98**, 2235–2248 (1995).
[26] M. B. Porter, The KRAKEN normal mode program. Rep. SM-245 (SACLANT Undersea Research Centre, La Spezia, Italy), 1991.
[27] W. A. Kuperman, ''Coherent component of specular reflection and transmission at a randomly rough two-fluid interface,'' J. Acoust. Soc. Am. **58**, 365–370 (1975).
[28] C. Bender and S. Orszag, *Applied Mathematical Methods for Scientists and Engineers* (McGraw-Hill, New York, 1978).